20 May 1994

ELSEVIER

Chemical Physics Letters 220 (1994) 371–377

CHEMICAL PHYSICS LETTERS

Non-Cartesian sampling schemes and the acquisition of 2D NMR correlation spectra from single-scan experiments

Lucio Frydman [1], Jian Peng

Department of Chemistry (M/C 111), University of Illinois at Chicago, Chicago, IL 60607-7061, USA

Received 1 February 1994

Abstract

Continuous non-Cartesian sampling schemes, widely used in modern NMR imaging, can yield complete 2D NMR spectra within a single-scan signal digitization. The present work illustrates a purely spectroscopic application of this strategy to the extraction of 2D NMR spectra from heteronuclear pairs of coupled spins. The experiment allows one to digitize a unidimensional data set which after proper rearrangement and processing, affords a complete chemical shift-heteronuclear coupling 2D correlation NMR spectrum. Theoretical and computational aspects involved in these single-scan experiments are discussed, and a series of solution NMR examples are presented.

1. Introduction

The extremely wide range of applications spanned by modern multidimensional NMR spectroscopy reflects the remarkable insight and ingenuity with which these techniques were originally proposed [1,2]. In 2D NMR for instance, the well-known experimental scheme [2–4]

preparation–evolution (t_1)–

mixing–detection (t_2) (1)

is general enough to achieve a wide variety of different goals, ranging from the separation of overlapping peaks to the indirect detection of 'forbidden' spin coherences. Such versatility results from the different roles that each of the time periods in the pulse-sequence (1) plays in the data acquisition [2–6]. During the initial preparation period spins are taken away from equilibrium and transformed into a coherent state, which evolves under the effects of an initial Hamiltonian $\mathscr{H}_1$ for a time period t_1. The resulting coherences are subsequently transformed by suitable mixing pulse sequences into observable transverse spin magnetizations, whose macroscopic signals are digitized as a function of t_2 while evolving under the effects of a second Hamiltonian $\mathscr{H}_2$. This procedure is repeated several times for stepwise incremented evolution periods until an adequate bidimensional signal $S(t_1, t_2)$ is collected. Then, a faithful approximation to the correlation distribution between states that started precessing at certain Bohr frequencies of $\mathscr{H}_1$ and were transferred by the mixing into single-quantum coherences evolving under the effects of $\mathscr{H}_2$, can be retrieved as

$$I(\Omega_1, \Omega_2) = \int \mathrm{d}t_1 \exp(-\mathrm{i}\Omega_1 t_1) \times \int \mathrm{d}t_2 \exp(-\mathrm{i}\Omega_2 t_2) S(t_1, t_2) \,. \quad (2)$$

It is the calculation of this $I(\Omega_1, \Omega_2)$ spectral distri-

[1] Lucio Frydman is a Camille and Henry Dreyfus New Faculty Awardee (1992–1997).

SSDI 0009-2614(94)00359-X

bution what constitutes the final goal of 2D NMR spectroscopy.

The remarkable generality of this approach results from the fact that regardless from the type of interactions being correlated or from the nature of the transfer taking place during the mixing, the time-domain evolution of *all* spins involved can be described by a single set of orthogonal trajectories like the one illustrated in Fig. 1A. Indeed, in all pulse schemes that conform to Eq. (1), the well-defined time evolution phases

$$\phi = \Omega_1 t_1 + \Omega_2 t_2 , \tag{3}$$

that develop allow one to extract the $I(\Omega_1, \Omega_2)$ distribution by Fourier analysis of the scanned bidimensional signal with respect to the extraction vector (t_1, t_2) [3]. It is important to note however that there are no a priori reasons for constraining the sampling of a bidimensional time-domain space to sequential orthogonal trajectories. If relaxation and other dissipative processes can be disregarded, the phases

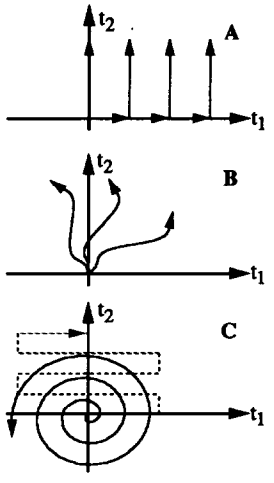

Fig. 1. Graphical representation of different time-domain approaches capable of affording the data required for retrieving 2D NMR spectra. (A) Cartesian approach normally used in conventional 2D NMR. (B) Non-Cartesian sampling involving the evolution of the spins under the simultaneous effects of two interactions whose mutual correlation is being sought. (C) Arbitrary trajectories which use time as a parameter for continuously sampling large regions of a bidimensional time-domain space within a single scan. The continuous curve represents a case where both interactions can be refocused; the dashed curve would result if only one of the interactions were refocused while the second is intermittently averaged out.

evolved by spin coherences for a given coordinate (t_1, t_2) of the time domain are independent of how the system actually arrived to that point. Therefore, general sampling schemes can also include non-Cartesian trajectories like those depicted in Fig. 1B, representing the evolution of an excited spin system as a function of arbitrary 'proportions' of $\mathscr{H}_1$ and $\mathscr{H}_2$. These ways of sampling the time domain are usually unable to distribute the digitized data over a dense rectangular grid of points ready to be fast Fourier transformed. They may however compensate for this computational drawback, by opening new vistas regarding the design of more flexible acquisition sequences for the collection of experimental data. Indeed starting from the original Lauterbur experiment itself, which involved the sampling of a multidimensional space along diagonal trajectories [7], several magnetic resonance imaging (MRI) [8,9] and spectroscopic NMR techniques [10,11] have exploited the advantages of this kind of strategy.

Departing from conventional 2D sampling schemes can also lift the requirement for an independent t_1 evolution period in charge of encoding one of the interactions. Instead, the acquisition time of the experiment can be used *as a trajectory parameter* for sampling large volumes of multidimensional time-domain spaces within a single signal digitization. Such scanning principle was originally proposed by Mansfield and co-workers, and lies at the core of ultrafast echo-planar techniques that provide detailed MRI images within fractions of a second [12,13]. Using a heteronuclear coupled pair of spins as model case, we exemplify here how the advantages of this type of sampling schemes can also be incorporated into purely spectroscopic NMR experiments. Section 2 introduces a multiple-pulse irradiation sequence that encodes all the information required to retrieve a complete chemical shift-heteronuclear coupling 2D NMR spectrum within a continuous single-scan acquisition. The data processing involved in the resulting multiple-echo single-scan spectroscopy (MESSY) technique is described, and illustrated with applications to the fast acquisition of 2D solution NMR spectra.

2. Theory and data processing

Consider a non-relaxing spin system capable of evolving under the effects of two interactions whose mutual correlation is being sought. Fig. 1C illustrates the basic types of manipulations which could allow one to acquire all the information required to calculate such 2D NMR spectrum within a single scan. The dashed curve corresponds to a situation where one of the interactions is periodically refocused while the second only acts for certain periods of time. Whether data sampled along this trajectory are complete enough to faithfully yield all the frequency information will depend on the particular features of the 2D spectral distribution, as well as on the possibility of shifting the acquisition trajectory around the time-domain origin. If on the other hand *both* interactions can be independently refocused throughout the 1D signal acquisition without significant intensity losses (continuous curve in Fig. 1C), the complete collection of adequate $S(t_1, t_2)$ bidimensional data sets within a single scan becomes feasible in general. One of the simplest systems where the latter situation is realized consists of a spin S (e.g., ^{13}C) interacting either via dipolar or indirect coupling with a group of isolated heteronuclei (e.g., protons). We focus therefore on the rotating-frame Hamiltonian $\mathscr{H}$ of S,

$$\mathscr{H} = -\Delta\Omega S_z + \Omega_{IS} I_z S_z \,, \tag{4}$$

where $\Delta\Omega$ includes the chemical shift and resonance offset of S, and Ω_{IS} characterizes the I–S coupling interaction. After conventional excitation the time evolution of the S-spin ensemble is dictated by the exponential operator $\mathscr{U}(t)$,

$$\mathscr{U}(t) = \exp(-i\mathscr{H}t)$$

$$= \exp(i\Delta\Omega S_z t)\exp(-i\Omega_{IS} I_z S_z t) \,, \tag{5a}$$

$$= \mathscr{U}_S(t)\,\mathscr{U}_{IS}(t) \,, \tag{5b}$$

which can be factorized in terms of shift and coupling evolution operators $\mathscr{U}_S(t)$, $\mathscr{U}_{IS}(t)$ thanks to the fact that both terms in Eq. (4) commute. Although the free time evolution of the S spins cannot distinguish among Bohr frequencies of shift and coupling Hamiltonians, these can be discerned by the application of π pulses [14]. The effects that the rotations R associated to these pulses have on the spins can be taken into account by computing an effective interaction Hamiltonian $\bar{\mathscr{H}}$, obtained from the rotating-frame Hamiltonian by the transformation [15]

$$\bar{\mathscr{H}} = R \cdot \mathscr{H} \cdot R^{-1} \,. \tag{6}$$

Ideally, a π-pulse rotation applied at the Larmor frequency of a spin will change the sign of the corresponding longitudinal spin operators in the Hamiltonian. Thus, $(\pi)_S$ pulses on-resonance with the S-spin precession will reverse the signs of both the shift and the coupling terms in $\mathscr{H}$; $(\pi)_I$ pulses at the Larmor frequency of the I spin will only reverse the sign of the coupling part; and simultaneous $(\pi)_S$, $(\pi)_I$ pulses will reverse the shift while leaving unchanged the coupling term of $\mathscr{H}$. These changes in sign will lead to the refocusing of the different interactions and create spin-echo phenomena; their effects therefore can be represented by a reversal in the direction of the time axis determining the evolution of excited coherences [16]. Since depending on the type of pulse irradiation being used shift and coupling interactions will be affected in different ways, it is convenient to label these time reversals by two independent time variables. Using t_S and t_{IS} to denote these parameters, the effects of pulses on the total time development operator can be represented as

$$\mathscr{U}_S(t_S)\,\mathscr{U}_{IS}(t_{IS}) \xrightarrow{(\pi)_S} \mathscr{U}_S(-t_S)\,\mathscr{U}_{IS}(-t_{IS}) \,, \tag{7a}$$

$$\mathscr{U}_S(t_S)\,\mathscr{U}_{IS}(t_{IS}) \xrightarrow{(\pi)_I} \mathscr{U}_S(t_S)\,\mathscr{U}_{IS}(-t_{IS}) \,, \tag{7b}$$

$$\mathscr{U}_S(t_S)\,\mathscr{U}_{IS}(t_{IS}) \xrightarrow{(\pi)_S,(\pi)_I} \mathscr{U}_S(-t_S)\,\mathscr{U}_{IS}(t_{IS}) \,. \tag{7c}$$

According to these equations evolution always begins along the $t_S = t_{IS} = t$ curve, t being the actual physical time elapsed since excitation. Radiofrequency irradiation however affects the trajectory followed by the spins in different ways, reversing the signs of t_S or of t_{IS} depending on which of the interactions is being refocused.

The signal S detected from the total spin ensemble as a function of its coordinate in the (t_S, t_{IS}) space is given by the sum over all possible shift and couplings in the system of a series of oscillating coherences,

$$S(t_S, t_{IS}) = \int\int I(\omega_S, \omega_{IS})$$

$$\times \exp[i(\omega_S t_S + \omega_{IS} t_{IS})]\, d\omega_S\, d\omega_{IS} \,, \tag{8}$$

where ω_S and ω_{IS} are, respectively, Bohr frequencies of the shift and coupling Hamiltonians. The weighting coefficient $I(\omega_S, \omega_{IS})$ describes the probability of having spins evolving simultaneously at shift frequencies ω_S and at coupling frequencies ω_{IS}, and represents the 2D NMR spectrum separating the I–S couplings in the system according to the chemical shifts of different S sites [17,18]. Eqs. (2) and (8) indicate that this spectral distribution can become available from $S(t_S, t_{IS})$ by 2D Fourier analysis, provided that the signal over a large enough region of the (t_S, t_{IS}) time-domain space were sampled. One possibility for implementing such sampling is to carry out several independent experiments where, following the initial excitation, single $(\pi)_I$ or $(\pi)_I$, $(\pi)_S$ pulses are placed at a series of regularly incremented times t_1. This is the kind of acquisition involved in conventional 2D NMR. The sampling flexibility illustrated by Eqs. (7) however opens up the possibility of using the physical acquisition time t as a parameter, capable of encoding the behavior of the spins over an arbitrarily large region of (t_S, t_{IS})-space in a single scan. Indeed consider the effects of a multiple pulse sequence like the one illustrated in Fig. 2A, composed by an initial excitation followed by a series of alternating $(\pi)_I$ and $(\pi)_I$, $(\pi)_S$ pulses. If the time delays separating these pulses are increased throughout the sequence in a pairwise and linear fashion, spins will evolve in the (t_S, t_{IS}) space along a continuous outward-expanding trajectory like the one illustated in Fig. 2B. Other than relaxation no factors will limit the number of shift and coupling echoes that can be involved; signal sampled during such a pulse sequence should therefore provide enough information to yield a complete shift-coupling 2D NMR spectrum without suffering from any obvious resolution complication.

Although the multiple-pulse sequence shown in Fig. 2A can encode a complete 2D time-domain set of signals within a single continuous acquisition, it is unable to distribute the digitized data over a dense grid of points ready to be fast Fourier transformed. This problem can be partially solved by monitoring the signal at constant digitization rates $1/\Delta t$; Δt being the amount of time by which the separation between π-pulses is incremented throughout the sequence. As illustrated in Fig. 2C, all points acquired during such an experiment correspond to integer coordinates of a

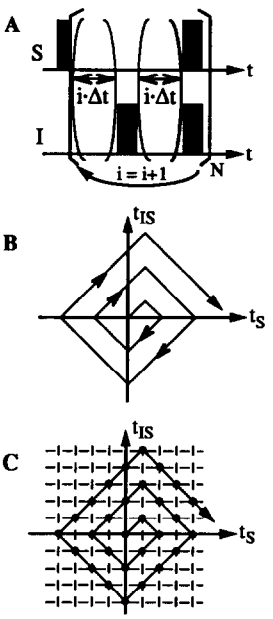

Fig. 2. Different aspects involved in the recording of 2D J heteronuclear NMR spectra via a single-scan acquisition. (A) Multiple-pulse sequence capable of affording the required series of alternating shift and coupling time-domain echoes. It consists of an initial S pulse excitation, followed by a series of $(\pi)_I$ and $(\pi)_I$, $(\pi)_S$ pulses whose separation increases linearly as $i\Delta t$; $i = 1, 2, ..., N$. (B) Trajectory followed by the S spins in the (t_S, t_{IS}) space, as driven by the pulse sequence shown on the top scheme. (C) Strategy employed for obtaining a dense bidimensional grid of equally-spaced points (represented by the dashed lines) from the 1D signal sampled during the multiple-pulse sequence shown in part (A) (continuous curve). Filled dots correspond to data positions sampled during the single-scan acquisition; the remaining positions of the grid can either be directly monitored during a second experiment or, as was done in the present study, they can be estimated by numerical methods.

regular bidimensional lattice. Only half the positions in this lattice can be probed by the acquisition of a single scan; the behavior of the spins at the remaining positions can either be directly monitored by performing a second scan using slightly different initial conditions (waiting time delays $\frac{1}{2}\Delta t$ instead of Δt between the first pair of pulses), or estimated by interpolation of the time-domain signal already available. We decided to implement this second alternative, which is particularly straightforward due to the fact that each grid point (i, j) to be interpolated is flanked along its t_S and t_{IS} coordinates by four equidistant grid positions where data have been sampled. Bilinear in-

terpolation of the signal $S_{i,j}$ at the undetected points can then be carried out as

$$S_{i,j} = \tfrac{1}{4}(S_{i+1,j} + S_{i-1,j} + S_{i,j+1} + S_{i,j-1}) , \qquad (9)$$

where all the complex signals on the right-hand side of the equation are known.

Acquisition times along the t_S and t_{IS} dimensions are determined by the total number of pulses used, as well as by the separation between digitized data points. These acquisition times should be chosen long enough to support a significant decay of the signal, so as to avoid artifacts originating from time-domain data truncation. This choice also helps to alleviate one of the main limitations of the experiment, arising from the fact that the procedure described above yields equal dwell times along both time axes. By having the opportunity to acquire data over a large time-domain region it is possible to characterize small coupling constants even in the presence of large spectral widths, chosen to accommodate the chemical shift dispersion of widely inequivalent sites.

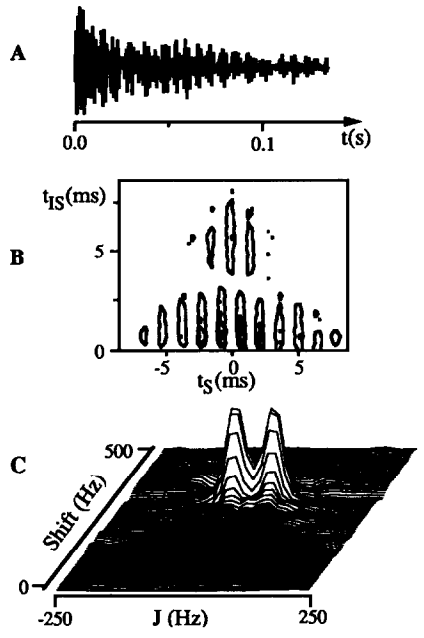

Fig. 3. Different stages leading to the 2D J heteronuclear correlation spectrum of benzene from a 1D time-domain NMR signal. (A) Experimental ^{13}C NMR data acquired using a multiple-echo sequence similar to the one shown in Fig. 2A; 528 points (real part shown) were digitized with a dwell time separation $\Delta t = 250$ μs after an NOE buildup of 2 s. (B) Magnitude contour plot of the bidimensional set obtained after rearranging and interpolating the experimental data over a 32×63 2D matrix of equidistant points. (C) Expanded region of the 2D shift-heteronuclear coupling spectrum obtained after zero-filling the set shown in plot (B) to 64×128 points and 2D Fourier processing. The origin along the shift axis corresponds to the transmitter carrier frequency.

3. Experimental

To verify the predictions of the preceding paragraphs, a series of ^{13}C solution NMR experiments on model ^{13}C–^{1}H J-coupled systems were carried out. All chemicals were purchased from Fisher Scientific and used without further purification. A home-built NMR spectrometer based on a 7.08 T superconducting magnet and on Tecmag pulse-programmer and data acquisition systems was used. Data rearrangement, interpolation, and processing were carried out on the same Macintosh Quadra computer that controls the spectrometer's operation. The processing used in the actual implementation of the experiments was similar to the one described in the previous paragraph. Due to instrumental limitations however, signal digitization was restricted to the time-domain half-plane corresponding to positive values of t_{IS}.

4. Results and discussion

Fig. 3 illustrates results obtained with the MESSY procedure described above on a sample of neat C_6H_6. Part (A) shows the unidimensional data acquired using a spiral trajectory with sixteen 'windings' around the origin and a total signal averaging of four scans, phased-cycled so as to eliminate baseline and ghost artifacts. After rearranging these data in their proper (t_S, t_{IS})-space positions and interpolating them over a dense grid of equally spaced points, the bidimensional set illustrated in Fig. 3B was obtained. At this stage treatment of the time-domain data can proceed as in conventional 2D echo NMR [3]; apodization, zero filling, 2D fast Fourier transform and phasing lead to the chemical shift-heteronuclear coupling 2D correlation NMR spectrum illustrated in Fig. 3C. This distribution shows all the features that could have been predicted from the coupling and offset parameters of the ^{13}C site, including essentially purely absorptive line shapes which become available due to

the presence of an effective time-domain chemical shift echo. Fig. 4 shows additional results obtained with the multiple-pulse sequence on a dioxane/methanol mixture. Both the chemical shift differences as well as the different number of protons coupled to the two inequivalent types of carbons are evident from the spectral features. Finally, Fig. 5 illustrates the results that were obtained when MESSY was applied on a sample of neat pyridine. The chemical nature of the inequivalent carbons in the molecule as well as their J couplings to the directly bonded protons are evident from the 2D NMR spectrum, *obtained as a result of collecting a single ^{13}C NMR scan and requiring a total acquisition time of 202.2 ms.*

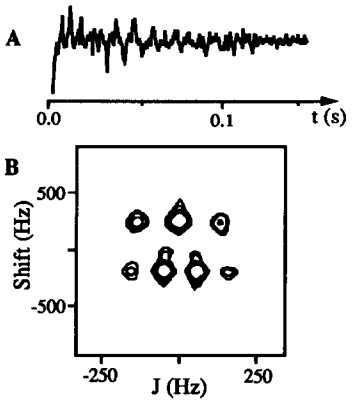

Fig. 4. (A) Unidimensional ^{13}C NMR data set obtained with the MESSY sequence on a 1/1 dioxane/methanol mixture. A dwell time $\Delta t = 300$ μs was used; other experimental acquisition parameters are as in Fig. 3. (B) Expanded region of the 2D correlation NMR spectrum retrieved after rearrangement and Fourier processing of the 1D data.

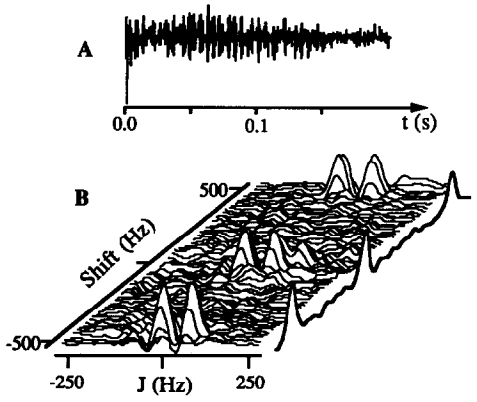

Fig. 5. (A) Single ^{13}C NMR scan acquired on a pyridine sample with a multiple-pulse MESSY sequence, using a (t_S, t_{IS})-space trajectory involving 15 'windings' around the origin. 465 (points separated by 435 μs dwell times were acquired in this experiment. (B) Zoomed region of the 2D NMR spectrum obtained after processing the single-scan data shown in part (A). The plot on the right is the chemical shift projection, reflecting the proton-decoupled signal arising from the three inequivalent sites in the molecule.

The most significant spectroscopic aspect of multiple-echo pulse sequences like the one described above is their capability to provide large amounts of multidimensional time-domain NMR data within a single-scan acquisition. This advantage may be especially useful when trying to establish multidimensional correlations among three or more frequency interactions, or when trying to characterize transient chemical systems in real time. An improvement over the conventional scheme of acquiring 2D NMR data can already be achieved if only one of the interactions can be refocused. It was indeed on the basis of this premise that Bax and co-workers proposed their shift-echo scheme for the improved recording of homonuclear J correlation spectra [19]. We trust that with the advanced arsenal of spin- and spatial-manipulation tools currently available in NMR, it will be possible to extend the applications of these strategies to the extraction of chemical correlations among other kinds of solid- and solution-state NMR interactions. Then, there are in principle no reasons for preventing continuous single-scan acquisition schemes of achieving within the field of spectroscopic NMR an impact comparable to the one that they already have in clinical NMR imaging.

Acknowledgement

We are very grateful to Dr. Lyndon Emsley (Centre de Etudes Nucleaires de Grenoble) and to Professor Alex Pines (University of California–Berkeley) for their simulating suggestions and discussions. The instrumentation used in the present work was supported in part by the University of Illinois at Chicago; acknowledgment is also made to the donors of the Petroleum Research Fund administered by the ACS for partial support of this research.

References

[1] J. Jeener, Ampere International Summer School II (Basko Polje, 1971).

[2] W.P. Aue, E. Bartholdi and R.R. Ernst, J. Chem. Phys. 64 (1976) 2229.

[3] R.R. Ernst, G. Bodenhausen and A. Wokaun, Principles of nuclear magnetism in one and two dimensions (Oxford Univ. Press, Oxford, 1987).

[4] H. Kessler, M. Gehrke and C. Griesinger, Angew. Chem. Intern. Ed. Engl. 27 (1988) 490.

[5] A. Bax, Two-dimensional nuclear magnetic resonance in liquids (Delft Univ. Press, Delft, 1982).

[6] A.E. Derome, Modern NMR techniques for chemistry research (Pergamon Press, Oxford, 1987).

[7] P.C. Lauterbur, Nature 242 (1973) 190.

[8] P.T. Callaghan, Principles of nuclear magnetic resonance spectroscopy (Oxford Univ. Press, Oxford, 1991).

[9] P. Mansfield and P.G. Morris, NMR imaging in biomedicine (Academic Press, New York, 1982).

[10] L. Frydman, G.C. Chingas, Y.K. Lee, P.J. Grandinetti, M.A. Eastman, G.A. Barrall and A. Pines, J. Chem. Phys. 97 (1992) 4800.

[11] L. Frydman, G.C. Chingas, Y.K. Lee, P.J. Grandinetti, M.A. Eastman, G.A. Barrall and A. Pines, Israel J. Chem. 32 (1992) 161.

[12] P. Mansfield, J. Phys. C 10 (1977) L55.

[13] M.K. Stehling, R. Turner and P. Mansfield, Science 254 (1991) 43.

[14] C.P. Slichter, Principles of magnetic resonance (Springer, Berlin, 1990).

[15] M. Mehring, High resolution NMR in solids (Springer, Berlin, 1983).

[16] W. Rhim, A. Pines and J.S. Waugh, Phys. Rev. B 3 (1971) 684.

[17] G. Bodenhausen, R. Freeman and D.L. Turner, J. Chem. Phys. 65 (1976) 839.

[18] L. Müller, A. Kumar and R.R. Ernst, J. Chem. Phys. 63 (1975) 5490.

[19] A. Bax, A.F. Mehlkopf and J. Smidt, J. Magn. Reson. 40 (1980) 213.